JOURNAL OF AGRICULTURAL AND FOOD CHEMISTRY
ARTICLE

J. Agric. Food Chem. 2010, 58, 11653–11661 11653
DOI:10.1021/jf1031668

Luteolin Ameliorates Experimental Lung Fibrosis Both *in Vivo* and *in Vitro*: Implications for Therapy of Lung Fibrosis

Chiu-Yuan Chen,[†] Wen-Huang Peng,[‡] Li-Chen Wu,[§] Chun-Chi Wu,[∥] and Shih-Lan Hsu*,[†,§,∥,⊥]

[†]Graduate Institute of Natural Healing Sciences, Nanhua University, Chia-Yi 622, Taiwan, [‡]Graduate Institute of Chinese Pharmaceutical Sciences, China Medical University, Taichung 404, Taiwan, [§]Department of Applied Chemistry, National Chi-Nan University, Puli, Nantou 545, Taiwan, [∥]Institute of Medical and Molecular Toxicology, Chung Shan Medical University, Taichung, Taiwan, and [⊥]Department of Education & Research, Taichung Veterans General Hospital, Taichung 407, Taiwan,

Lonicera japonica (*Caprifoliaceae*) has been known as an anti-inflammatory herb in traditional Chinese medicine for thousands of years and is used constantly for upper respiratory tract infections. Luteolin, an active flavonoid compound isolated from *Lonicera japonica*, has a spectrum of biological activities, especially with antioxidative and anti-inflammatory properties. However, whether luteolin has a direct inhibitory effect on lung fibrosis has not been established. In this study, we examined the effects of luteolin on lung fibrosis both *in vivo* and *in vitro*. We found that oral administration of luteolin (10 mg/kg) efficiently suppressed the neutrophil infiltration as well as TNF-α and IL-6 elevation in the bronchoalveolar lavage fluid in bleomycin-instilled C57BL/6J mice. Luteolin also alleviated collagen deposition, TGF-β1 expression, and lung fibrosis upon bleomycin instillation. A similar tendency was observed in both early and delayed luteolin-treated groups. Next, our *in vitro* studies showed that luteolin inhibited TGF-β1-induced α-SMA, type I collagen, and vimentin expression in primary cultured mouse lung fibroblasts. Moreover, luteolin significantly blocked TGF-β1-mediated epithelial marker (E-cadherin) downregulation and mesenchymal cell markers (fibronectin and vimentin) upregulation, as well as retaining epithelial morphology in human alveolar epithelial-derived A549 cells. Additionally, luteolin could attenuate TGF-β1-induced Smad3 phosphorylation in both lung fibroblasts and A549 cells. These findings suggest that luteolin has a potent antifibrotic activity; this effect was mediated, at least in part, by inhibition of lung inflammation and suppression of myofibroblast differentiation as well as epithelial-to-mesenchymal transition.

KEYWORDS: Luteolin; bleomycin; lung fibrosis; TGF-β1; epithelial-to-mesenchymal transition

INTRODUCTION

Interstitial lung disease (ILD) is a broad category of lung diseases that includes more than 130 disorders which are characterized by fibrosis and inflammation of the lungs. Much work has been done in an attempt to explain the etiology of ILDs, such as occupational/environmental factors, drugs, hypersensitivity reactions and infections (*1*). Although ILDs can develop from a variety of sources, the disease processes, including cell repair, immune responses, fibroblast proliferation and increased secretion of collagen and extracellular matrix, all share the same characteristics with formation of lung fibrosis (*2*). Previous studies reported that several factors play important roles in the development of fibrosis including profibrotic cytokines, chemokines, eicosanoids, fibrinolytic/fibrinogenic factors, oxidative stress, matrix metalloproteinases and their inhibitors (*2*). Among them, transforming growth factor beta 1 (TGF-β1), a potent profibrotic cytokine, is one of the central mediators which induce the phenotypic modulation of fibroblasts to myofibroblasts, which have the potential to play important roles in the pathogenesis of pulmonary fibrosis and to contribute to the recruitment of inflammatory cells (*3*). Histological evaluation of lung tissue further shows evidence of inflammation and disorder of lung mesenchymal cells in patients and experimental animals with lung fibrosis (*4*, *5*). Moreover, a number of studies on the pneumonia/lung fibrosis mechanism have documented that inflammatory cells such as macrophages, lymphocytes and neutrophils play a key role in secretion of a variety of cytokines and growth factors that regulate proliferation, chemotactism and secretory activity of fibroblasts (*6*). These observations suggested that the inflammatory process results in lung injury and lung fibrosis and emphasized that effective therapies for these disorders must be given early in the natural history of the disease, prior to the development of extensive lung destruction and fibrosis. The drug therapies, such as steroids, immunosuppressor, and antifibrosis drug (colchicine), that are currently available for ILDs can have serious side effects and often are not effective. Hence, new drugs

*To whom correspondence should be addressed. Tel: 886-4-23592525 ext 4037. Fax: 886-4-23592705. E-mail: h2326@vghtc.gov.tw.

Published on Web 10/19/2010

with a higher therapeutic effect and lower side effects are urgently needed for these patients.

It is noteworthy that the use of medicinal plants or their active components is becoming an increasingly attractive approach for the complementary and alternative treatment of various inflammatory disorders. *Lonicera japonica* (*Caprifoliaceae*) has been known as an anti-inflammatory herb in traditional Chinese medicine for thousands of years, and is widely used for upper respiratory tract infections and rheumatoid arthritis. It was also used for treatment of severe acute respiratory syndrome (SARS) in Mainland China (*7*). Luteolin (3′,4′,5,7-tetrahydroxyflavone), an active flavonoid compound isolated from *Lonicera japonica*, is widely distributed in the plant kingdom. Preclinical studies have shown that this flavone possesses a variety of pharmacological activities, including antioxidant, anti-inflammatory, antimicrobial, and anticancer activities (*8*). Recently, luteolin has been found to alleviate bronchoconstriction and airway hyperreactivity in ovalbumin sensitized mice (*9*). It also can decrease the acute *Chlamydia pneumoniae* infection load and inflammatory reactions in lung tissue of treated mice (*9*, *10*). Our previous report further demonstrated that luteolin suppresses inflammation-associated gene expression by blocking NF-κB and AP-1 activation pathways in mouse alveolar macrophages (*11*). However, the therapeutic potential of luteolin for fibrotic lung diseases remains unclear. Interestingly, alveolar epithelial cells have been shown to undergo the epithelial−mesenchymal transition (EMT) to produce myofibroblasts in idiopathic pulmonary fibrosis patients, a mouse lung fibrosis model, and TGF-β1 treated A549 adenocarcinomic human alveolar basal epithelial cells (*12*).

In the current study, we examined the antifibrotic effects of luteolin in both *in vivo* and *in vitro* models. The effects of luteolin on the TGF-β1-stimulated fibroblast−myofibroblast transition and EMT of alveolar epithelial cells were examined on primary cultured mouse lung fibroblasts and human alveolar epithelial-derived A549 cell line *in vitro*. This is the first study to demonstrate that luteolin alleviates lung inflammation and fibrosis in bleomycin-instilled C57/BL6J mice, and inhibits the TGF-β1-stimulated myofibroblast differentiation and EMT *in vitro*.

MATERIALS AND METHODS

Chemicals and Reagents. Bleomycin was purchased from Nippon Kayaku (Tokyo, Japan). Luteolin was purchased from Extrasynthese (Genay, France). Prednisolone was purchased from NeWai Chemical Industrial Co. (Taiwan). Recombinant human TGF-β1 was purchased from R&D Systems (Minneapolis, MN). Antibodies and chemicals were obtained from the following sources: vimentin, α-smooth muscle actin (α-SMA) and FITC-conjugated goat anti-mouse IgG antibodies from Sigma (St. Louis, MO); collagen type I, Smad2/3 and p-Smad2/3 (ser433/435) antibodies from Santa Cruz Biotechnology (Santa Cruz, CA); E-cadherin antibody from BD Transduction Laboratories (San Jose, CA). RNA isolation kit and RT-PCR kit were obtained from GeneMark (Taiwan) and the PCR primers were synthesized by MDBIO, INC. (Taiwan).

Bleomycin-Induced Lung Fibrosis Model. Male C57BL/6 mice were obtained from National Laboratory Animal Center (Taipei, Taiwan), and 10-week-old mice were used in all experiments. All animal experiments were approved by the Animal Research Ethics Board of the Department of Education & Research, Taichung Veterans General Hospital (Taichung, Taiwan). C57BL/6 mice were randomly divided into six groups ($n = 10$ each group). Lung fibrosis was induced in male C57BL/6 mice by a single intratracheal instillation of 5 mg/kg of bleomycin in 0.3 mL of saline, and control mice received an equal volume of saline only. There are four groups of drug treatments: mice were orally administered daily with (1) luteolin (10 mg/kg, 1 mg/mL in ddH_2O) or (2) prednisolone (5 mg/kg, 1 mg/mL in ddH_2O) from day 1 to day 21 and mice were orally administered daily with (3) luteolin or (4) prednisolone from day 10 to day 21.

Bronchoalveolar Lavage Fluid Preparation and Cytokine Analyses. Bronchoalveolar lavage fluid was prepared by washing the lung four times with 4 mL of HBSS through a tracheal cannula. A 200 μL aliquot of the bronchoalveolar lavage fluid was placed in a cytospin and centrifuged at 500*g* for 5 min. The glass slides were Wright stained and subjected to a blinded manual cell count and differential. Cell differentials were counted with at least 200 leukocytes in each sample. The remaining bronchoalveolar lavage fluid was centrifuged at 300*g* for 5 min, and the supernatant was collected and stored at −70 °C for the cytokine analyses. TNF-α and IL-6 concentrations in BALF were measured using an ELISA kit (R & D systems, Minneapolis, MN) according to the manufacturer's standard protocol.

Pathological Examinations and Semiquantitative Pathological Index. Lung tissue was fixed by instilling 10% neutralized buffered formalin through the trachea, and embedded in paraffin. Three 4 μm thick transverse sections were stained with hematoxylin/eosin (Sigma) and Masson's Trichrome (DACO, Kyoto, Japan) using the manufacturer's standard protocol. Histologic grading of lesions was performed by using a blinded semiquantitative scoring system for extent of inflammation in lung parenchyma based on previous studies with minor modifications (*13*). Briefly, lung sections from animal were systematically scanned using a 20× objective lens, and 20 randomly selected fields were scored. The pathological features were determined based on (i) capillary congestion, (ii) intraalveolar and (iii) perivascular hemorrhage, (iv) interstitial, and (v) intraalveolar neutrophil infiltration. Each feature was scored from 0 to 4 according to its severity, and the score for each field was summed and averaged for each animal.

Fibrosis Quantitative Image Analysis. Fibrotic lung injury was assessed morphologically by quantitative image analysis (QIA). The degree of fibrosis was quantified by the Image-Pro Plus computer program (Media Cybernetics, Inc. Bethesda, MD) by analyzing slides as previously described with modifications (*14*). By adjusting image contrast, brightness, and color threshold settings, the image analysis program was configured to detect areas of blue stained collagen within each of 20 randomly selected fields per slide, captured using a 20× objective lens. The fraction of blue stained collagen areas for each field were summed and averaged for each animal. The area fraction of fibrosis is presented as mean ± SD.

Collagen Level Determination. Lungs were removed and homogenized in 1 mL of HBSS at day 21. Aliquots of lung homogenate were then assayed for total lung collagen levels and compared with a standard curve prepared from rat tail collagen by using the Sircoll collagen dye binding assay (BioColor Ltd., Newtownabbey, U.K.) according to the manufacturer's instruction.

RNA Extraction and Semiquantitative RT-PCR. Changes in TGF-β1 mRNA levels of mice lung after bleomycin stimulation were measured by semiquantitative RT-PCR. Total RNA was extracted from each specimen of lung tissue using Trisolution Reagent Plus (GeneMark, Taiwan) according to the manufacturer's instructions. For the amplification of the desired cDNA, the following gene-specific primers were used. TGF-β1: sense 5′-TGGACCGCAACAACGCCATCTATGAGAAAACC-3′, antisense 5′-TGGAGCTGAA GCAATAGTTGGTATCCAGGGCT-3′. Glyceraldehyde-3-phosphate dehydrogenase (GAPDH): sense 5′-TGGTATCGTGGAAGGACTCATGAC-3′, antisense 5′-ATGCCAGTGAGCTTCCCG TTCAG C-3′. The reaction conditions were set at 95 °C for 3 min followed by 25 to 30 cycles at 95 °C for 60s, 49 to 62 °C for 45s and 72 °C for 75s. The PCR products were subjected to separation on a 2% agarose gel and visualized by ethidium bromide staining and UV irradiation.

Cell Culture. Primary lung fibroblasts were isolated from 8 week old C57BL/6 mice, accomplished by using a protocol described previously with a slight modification (*14*). Briefly, the lungs were perfused via the pulmonary artery and lavage. Lung tissue was dissected from the airways, minced into 2-mm^3 pieces and digested with collagenase (1 mg/mL; Worthington) and 0.25% trypsin for 6 min. The digested lung tissues were filtered successively through a 22 μm nylon mesh and centrifuged at 300*g* for 5 min. The resulting pellets were plated on a Petri dish with Dulbecco's modified Eagle's medium (DMEM) supplemented with 10% fetal calf serum (FCS), 100 U/mL penicillin/streptomycin (Sigma) and 2 mM L-glutamine in a humidified incubator at 37 °C with 5% CO_2. Lung fibroblasts were purified by repeat trypsinization and passaging to achieve a homogeneous population. Identification of fibroblasts was based on the presence of α-SMA staining. A549 cells (ATCC, CCL-185) were cultured in DMEM supplemented with 100 U/mL penicillin/streptomycin and 10%

Table 1. Effects of Luteolin on Total and Differential Cell Count in BALF[a]

group	total cells ($\times 10^5$/mL)	differential cell count (%)		
		neutrophils	macrophages	lymphocytes
day 3				
control	0.38 ± 0.04	3.08 ± 0.65	94.36 ± 6.41	3.35 ± 0.56
BLM	$1.49 \pm 0.1^{\#}$	$29.48 \pm 3.27^{\#}$	$66.27 \pm 6.96^{\#}$	3.58 ± 0.81
BLM + Lut	$1.16 \pm 0.1^{\#*}$	$27.32 \pm 2.42^{\#*}$	$67.42 \pm 7.39^{\#}$	3.94 ± 0.57
BLM + Pred	$1.01 \pm 0.09^{\#*}$	$25.16 \pm 3.02^{\#*}$	$69.97 \pm 6.44^{\#}$	$4.41 \pm 0.73^{\#*}$
day 7				
control	0.41 ± 0.06	3.38 ± 0.85	92.54 ± 5.15	3.81 ± 0.47
BLM	$2.28 \pm 0.17^{\#}$	$21.07 \pm 2.43^{\#}$	$69.79 \pm 6.64^{\#}$	$8.75 \pm 1.17^{\#}$
BLM + Lut	$1.35 \pm 0.11^{\#*}$	$14.04 \pm 2.99^{\#*}$	$75.89 \pm 6.77^{\#*}$	$8.44 \pm 0.79^{\#}$
BLM + Pred	$1.43 \pm 0.18^{\#*}$	$12.36 \pm 2.54^{\#*}$	$76.92 \pm 10.37^{\#*}$	$8.76 \pm 1.12^{\#}$
day 14				
control	0.36 ± 0.07	2.84 ± 0.54	95.49 ± 5.15	3.53 ± 0.32
BLM	$1.45 \pm 0.15^{\#}$	$16.88 \pm 2.43^{\#}$	$74.72 \pm 3.48^{\#}$	$7.96 \pm 1.36^{\#}$
BLM + Lut	$1.01 \pm 0.09^{\#*}$	$10.48 \pm 2.13^{\#*}$	$79.89 \pm 6.77^{\#}$	$8.23 \pm 1.13^{\#}$
BLM + Pred	$0.96 \pm 0.11^{\#*}$	$11.68 \pm 1.65^{\#*}$	$77.72 \pm 9.66^{\#}$	$8.05 \pm 1.33^{\#}$

[a] Data presented as means ± SD of the group ($n = 10$). $^{\#}p < 0.05$ vs control. $^{*}p < 0.05$ vs BLM. BLM, bleomycin; Lut, luteolin; Pred, prednisolone.

FCS in a humidified incubator at 37 °C with 5% CO_2. For TGF-β1 experiments, cells were starved for 24 h using DMEM supplemented with 0.1% FCS before treatment.

Immunocytochemistry of Primary Cultured Lung Fibroblasts. Cells on coverslips were fixed for 5 min with 2% paraformaldehyde in phosphate buffered saline (PBS) and permeated with 1% Triton X-100/PBS for 15 min followed by washing twice with PBS. The coverslips were stained using α-SMA monoclonal antibody (mAb) overnight at 4 °C followed by FITC-conjugated anti-mouse IgG for 1 h. The coverslips were mounted on slides and visualized using confocal laser microscopy system (LSM 510-META; Carl Zeiss, Iena, Germany) with a water immersion objective lens for high resolution.

Western Blotting Analysis. Confluent cells (1×10^6) in a 10 cm Petri dish were treated with TGF-β1 (5 ng/mL) in the absence or presence of luteolin (25 μM). At each point in time, cells were washed with PBS and then scraped into microcentrifuge tubes and pellets. The cell pellets were resuspended in extraction lysis buffer and incubated for 20 min at 4 °C. Lysates (50 μg/lane) were separated by SDS−PAGE on polyacrylamide gels and transferred onto polyvinylidene difluoride membranes (PerkinElmer Life Sciences, Inc., Boston, MA). The membranes were probed with monoclonal primary antibody overnight at 4 °C. The blots were washed and incubated with horseradish peroxidase-conjugated rabbit anti-mouse or anti-rabbit IgG (1:20,000) for 1 h at room temperature. Following washing with TBST twice, immunoreactive bands were visualized using the ECL-Plus detection system (PerkinElmer Life Sciences, Inc., Boston, MA).

Statistical Analysis. All data are presented as mean ± SD. Statistical analysis among multiple groups was carried out by analysis of variance (ANOVA) followed by appropriate Tukey's tests including multiple comparison tests. All analyses were made using the SAS statistical software package and probability value of less than 0.05 were considered statistically significant. Student's *t*-test for pairs, considered significant at the $^{*}P < 0.05$, $^{**}P < 0.01$, or $^{***}P < 0.001$ level.

RESULTS

Anti-Inflammatory Action of Luteolin in Bleomycin-Instilled Mice. Male C57BL/6 mice were intratracheally instilled with 5 mg/kg of bleomycin or saline (control group), and then mice were untreated or orally administered daily with luteolin (10 mg/kg) or prednisolone (5 mg/kg) for indicated times. The lung inflammatory response after bleomycin administration was reflected by early increases of inflammatory cells in bronchoalveolar lavage fluid. As shown in **Table 1**, the total cells significantly increased in bronchoalveolar lavage fluid samples in the bleomycin-instilled group compared with the control group. Administration of luteolin and prednisolone effectively reduced the bleomycin-mediated increase in total cells and neutrophils proportion at day 7.

Elevation of TNF-α and IL-6 levels in bronchoalveolar lavage fluid is the sign of acute inflammation (*6*). To further confirm the anti-inflammatory action of luteolin, the levels of TNF-α and IL-6 were measured at days 3, 7, and 14 post bleomycin instillation. As depicted in **Figures 1A** and **1B**, the levels of TNF-α and IL-6 significantly increased in the bronchoalveolar lavage fluid of the bleomycin-instilled group. In contrast, treatment with luteolin and prednisolone reduced the levels of TNF-α and IL-6 in bleomycin-exposed mice. These data suggest that luteolin has an obvious anti-inflammatory function in bleomycin-instilled animals.

To further validate the effect of luteolin on anti-inflammatory function in mice treated with intratracheal bleomycin, histologic analysis of mouse lung tissue was performed. The bleomycin-instilled mice showed severe epithelial degeneration, inflammatory cell infiltrated in the alveoli and interstitium, and disrupted alveolar structure, at day 7 (**Figure 1C-b**). Inflammation in the air sacs of the lung leads to fluid leakage, and cellular breakdown was observed at 14 days after bleomycin instillation (**Figure 1C-f**). The destruction of the walls of the air sacs and the small blood vessels (capillaries) leads to the initiation of fibrotic processes. On the other hand, administrations of luteolin and prednisolone resulted in a strong amelioration of bleomycin-induced injury (**Figure 1C-c**,**d**,**g**,**h**). Furthermore, pathological grades of inflammation induced by bleomycin were significantly decreased in luteolin and prednisolone groups (**Figure 1D**) suggesting both luteolin and prednisolone effectively reduced the bleomycin-induced inflammatory injury.

Antifibrotic Effect of Luteolin in the Mouse Bleomycin Model. To examine the efficacy of luteolin and prednosolone to reduce fibrosis, mice were given an intratracheal instillation of bleomycin (day 0) to induce lung fibrosis, and then luteolin and predinosolone were administered once daily via oral gavage either from day 1 to day 21 (early treatment) or from day 10 to day 21 (delayed treatment). Animals were sacrificed at day 21 after treatment and the lungs were analyzed for the level of fibrosis by collagen deposition and TGF-β_1 expression profiling. Analyses of whole lung sections showed normal alveolar structure without fibrosis in the control group (**Figure 2A-a**). Mice instilled with bleomycin had profound fibrosis, both adjacent to the bronchi and at distal sites (**Figure 2A-d**). In contrast mice fed with luteolin and prednisolone significantly reduced levels of fibrosis (**Figure 2A-b**,**c**,**e**,**f**). Excessive deposition of an extracellular matrix, such as collagen, has been a hallmark of fibrosis. As shown in **Figure 2B**,

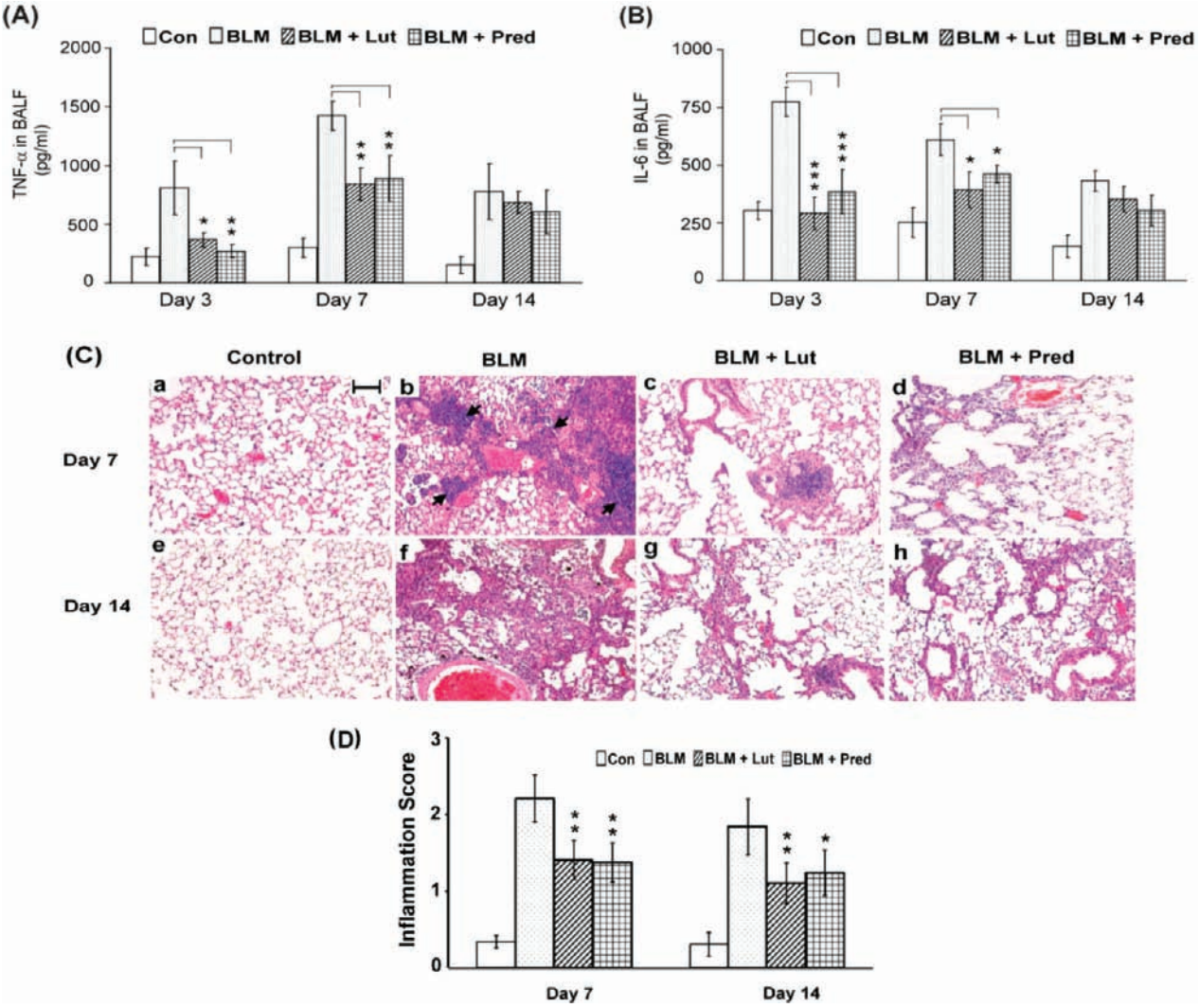

Figure 1. Luteolin ameliorated bleomycin-induced lung inflammatory injury. Mice were intratracheally instilled with 5 mg/kg of bleomycin or saline (control group), and then therapeutic groups were daily and orally treated with luteolin (10 mg/kg) or prednisolone (5 mg/kg) ($n = 10$). After 3, 7, and 14 days post bleomycin or saline treatment, bronchoalveolar lavage fluid was prepared as described in Materials and Methods. The levels of (**A**) TNF-α and (**B**) IL-6 in bronchoalveolar lavage fluid were measured. (**C**) Histophathology investigation. Lung tissues were collected and stained with hematoxylin/eosin staining. Images were selected according to the alveolitis scores. Bleomycin-instilled mice showed inflammation in the lung interstitium (**b**, arrows). Magnification 200×; scale bar, 100 μm. (**D**) Histological lesion scores of lung tissues from experimental groups as indicated in Materials and Methods. Data are presented as means ± SD of the group. *$p < 0.05$, **$p < 0.01$, compared with the BLM treatment. BLM, bleomycin; Lut, luteolin; Pred, prednisolone.

the area of lungs with collagen staining treated with bleomycin was 1.8- and 1.6-fold greater than in mice treated continuously with luteolin + bleomycin and prednisolone + bleomycin for 21 days (early treatment), respectively. Delayed treatment with prednisolone started at day 10 showed only slight reduction in fibrosis as suggested by the strong collagen staining. However, treatment of mice with luteolin from day 10 to day 21 still resulted in a strong reduction of collagen deposition. To examine the level of collagen accumulation in a more quantitative way, lungs from each group of mice at day 21 were assayed using the Sircoll collagen dye binding assay and total lung collagen levels were determined by comparing with a standard curve prepared from rat tail collagen. As shown in **Figure 2C**, bleomycin instillation significantly increased the collagen content of the lung by 5-fold, which represents the extent of fibrosis. Continuous treatment of mice with luteolin and prednisolone from day 1 to day 21 after bleomycin treatment (early treatment) resulted in a strong reduction of collagen accumulation (**Figure 2C**). Conversely, when treatment started at day 10 (delayed treatment), prednisolone showed no sign of reduction of collagen deposition. However, delayed treatment with luteolin still showed strong effect of blocking collagen accumulation (**Figure 2C**). To further demonstrate the antifibrotic ability of luteolin, the mRNA levels of TGF-β_1, a cytokine strongly involved in fibrogenic process, were measured in the lungs. The levels of TGF-β_1 in lungs significantly increased in the bleomycin-instilled mice, and early treatment of luteolin and prednisolone also showed a strong reduction of levels of TGF-β_1 (**Figure 2D**). Delayed treatment with prednisolone did not decrease the levels of TGF-β_1; however, delayed treatment with luteolin still exhibited the ability to block the expression of this fibrotic marker (**Figure 2D**). These findings implicate the antifibrotic effect of luteolin in both early inflammatory phase and late reparative phase and the potentially promising therapeutic activity of luteolin.

Luteolin Suppresses TGF-β_1-Induced Myofibroblastic Differentiation in Primary Cultured Lung Fibroblasts. Fibroblast proliferation and extracellular matrix accumulation play a critical role in the lung fibrogenic process. Among all the participating molecules, TGF-β_1 plays a key role in driving the differentiation of primary human pulmonary fibroblasts to myofibroblasts,

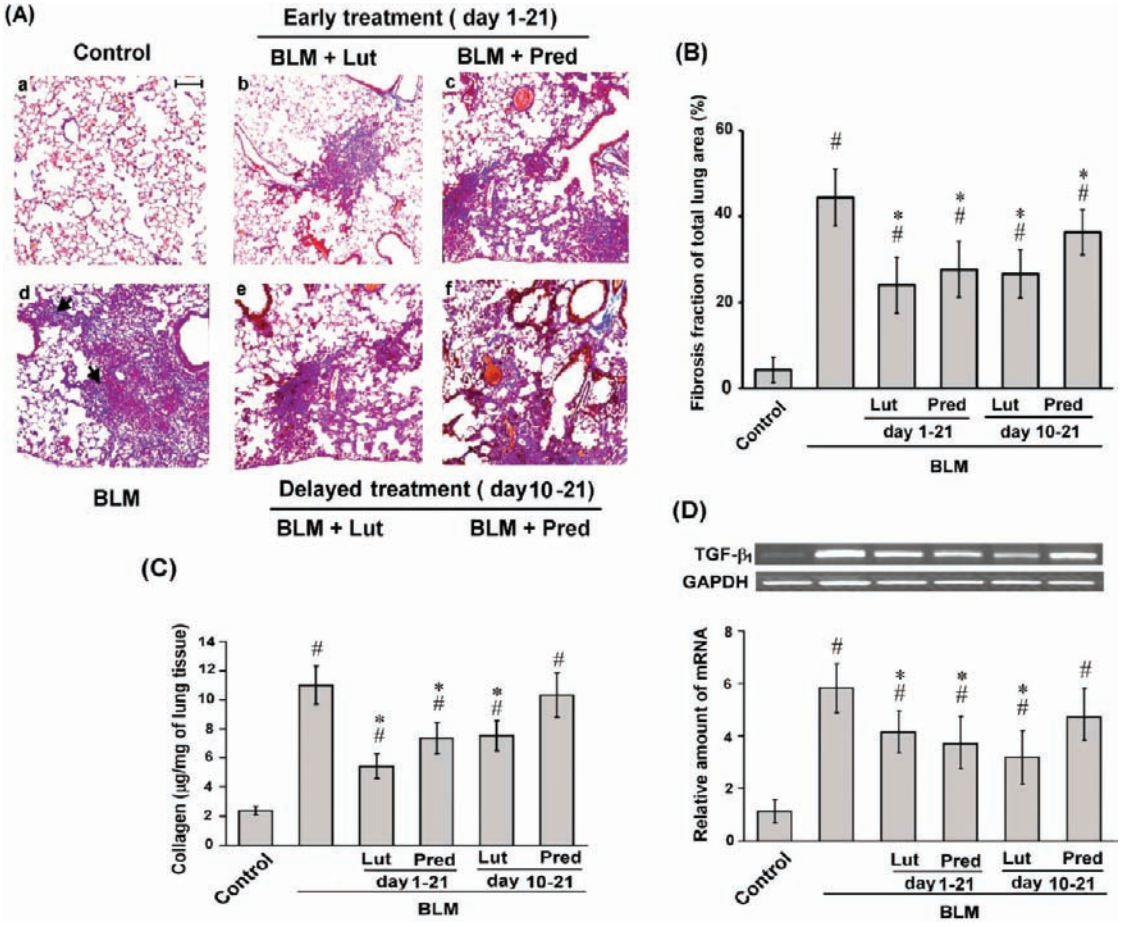

Figure 2. Luteolin alleviated bleomycin-induced lung fibrosis in mice. (**A**) Paraffin sections from day 21 mouse lungs were stained with Masson's Trichrome dye solution to show collagen deposition. Mice instilled with bleomycin had profound fibrosis, both adjacent to the bronchi and at distal sites (**d**, arrows). Magnification 200×; scale bar, 100 μm. (**B**) The fibrosis degree was quantified by the Image-Pro Plus computer program as described in Materials and Methods. (**C**) Collagen content in the lung tissue from experimental mice on day 21 was measured using a Sircol collagen kit as described in Materials and Methods. (**D**) TGF-β1 mRNA expression in the lung tissue from experimental mice was examined by RT-PCR analysis as described in Materials and Methods. Data are presented as means ± SD of the group (n = 10). #Significantly higher than control group (P < 0.05); *significantly lower than bleomycin treated mice (P < 0.05). BLM, bleomycin; Lut, luteolin; Pred, prednisolone.

promoting cell proliferation, and extracellular matrix deposition (*15*). To examine whether luteolin can inhibit cell proliferation and interfere with the transdifferentiation of myofibroblast induced by TGF-β_1, primary mouse lung fibroblasts were cultured with or without TGF-β_1 in the presence or absence of luteolin for indicated times (**Figure 3A**). As shown in **Figure 3A**, TGF-β_1 slightly accelerated the cell proliferation of primary mouse lung fibroblasts, whereas treatment with luteolin (25 μM) alone or cotreatment with TGF-β_1 significantly inhibited fibroblast proliferation.

Immunocytochemical analysis for myofibroblast marker α-SMA had shown that normal mouse primary lung fibroblast strains contained only few myofibroblasts (**Figure 3B**). However, upon treatment with TGF-β_1 (5 ng/mL) for 72 h, myofibroblast differentiation was promoted and cells expressed a large amount of α-SMA and had typical flattened myofibroblast morphology compared with the untreated cells (**Figure 3B**, TGF-β_1). With the addition of luteolin, TGF-β_1-induced morphological change and α-SMA expression were markedly suppressed (**Figure 3B**, Lut + TGF-β_1). To further confirm the transdifferentiation from fibroblasts to myofibroblasts, Western blot analyses were performed to detect the protein expressions of mesenchymal phenotype markers including α-SMA, collagen 1 and vimentin (**Figure 3C**). As expected, α-SMA, collagen 1, and vimentin significantly increased by TGF-β_1 treatment, while luteolin effectively inhibited TGF-β_1-induced α-SMA, collagen I and vimentin expression (**Figures 3C**).

Since activation of Smad pathway is the primary downstream signaling pathway of TGF-β_1 and changes in Smad protein expression have been implicated in bleomycin-induced lung fibrosis (*16*), we assessed the expression of total and phosphorylated Smad by immunoblot to further test the hypothesis that luteolin blocks the early step of TGF-β_1 signaling via the regulation of Smads. Primary mouse lung fibroblasts were pretreated with luteolin for 30 min and TGF-β_1 for another 30 min followed by Western blot. As shown in **Figure 3D**, total Smad2/3 were constitutively expressed in the primary mouse lung fibroblasts and were not affected by TGF-β_1 or luteolin treatment. However, the level of phosphorylated Smad2/3 was extremely increased by TGF-β_1 treatment and significantly inhibited by luteolin pretreatment. These observations suggest that luteolin blocks TGF-β_1-induced myofibroblast differentiation via inhibition of Smad activation.

Inhibition of TGF-β_1-Induced Epithelial-to-Mesenchymal Transition (EMT) by Luteolin in Human Alveolar Epithelial-Derived A549 Cells. Recent evidence from studies of fibrotic disorders supports a view that TGF-β_1 may play a novel role in pulmonary fibrogenesis by promoting alveolar epithelial cell transition to

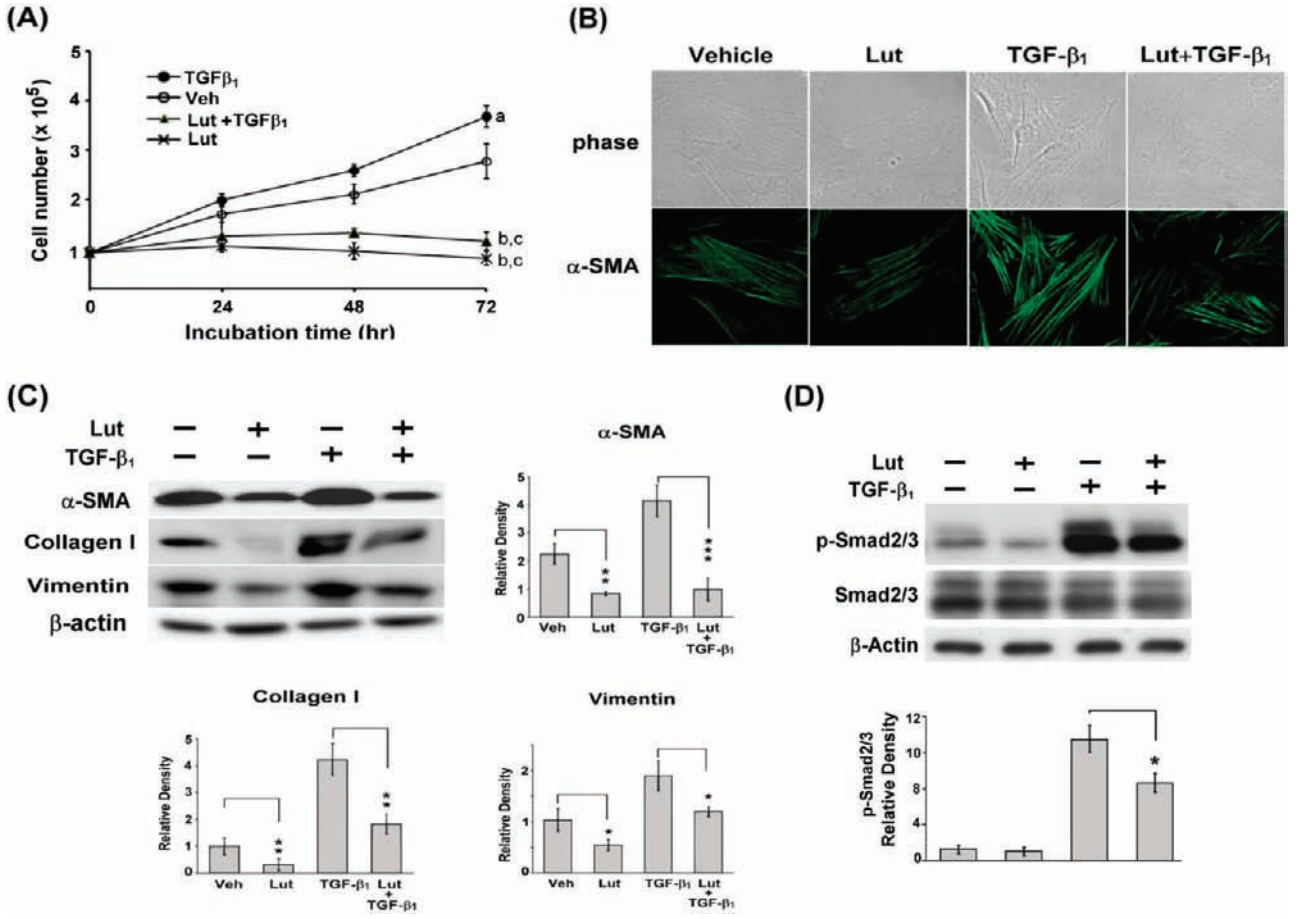

Figure 3. Luteolin suppressed TGF-β1-induced myofibroblastic differentiation in primary cultured lung fibroblasts. Serum-starved lung fibroblasts were induced with TGF-β1 (5 ng/mL) in the absence or presence of luteolin (25 μM) for 72 h. (**A**) Antiproliferative effect of luteolin in primary cultured lung fibroblasts. Cell number was evaluated by the trypan blue dye exclusion method. [a]Significantly higher than veh ($p < 0.05$); [b]significantly lower than veh ($p < 0.01$); [c]significantly lower than TGF-β1 ($p < 0.001$). (**B**) Luteolin decreased TGF-β1-induced α-SMA expression. α-SMA was immunocytochemically determined with anti-mouse α-SMA antibody (magnification 630×). (**C**) Western blot analysis was performed to detect α-SMA, vimentin and collagen protein expression in primary cultured lung fibroblasts. (**D**) Luteolin inhibited TGF-β1-induced Smad3 phosphorylation. Fibroblasts were pretreated with luteolin (25 μM), and then treated with TGF-β1 (5 ng/mL) for another 30 min. Phosphorylation and total Smad2/3 were measured by Western blot analysis using antibodies against phospho-Smad2/3 and Smad2/3. The blots were analyzed by densitometry and the results expressed as relative units. Data from triplicate experiments are shown as mean ± SD. *$p < 0.05$, **$p < 0.01$.

form mesenchymal cells with a myofibroblast-like phenotype (*17*). A549 cells, a human lung epithelial-derived cell line, also undergo an EMT in response to TGF-β_1, as evidenced by converting from an epithelial phenotype to a fibroblastic phenotype and loss of E-cadherin expression (*12*). To examine the effect of luteolin on TGF-β_1-induced alveolar EMT, A549 cells were stimulated with TGF-β_1 (5 ng/mL) in the absence or presence of luteolin (25 μM) for 48 h. As shown in **Figure 4A**, untreated A549 cells exhibited a cobblestone-like epithelial morphology and cell−cell adhesion is clearly observed. Cells grown in the presence of TGF-β_1 displayed a stellate and elongated fibroblast-like morphology and reduced cell−cell contact representing morphological changes associated with EMT. For combined treatment of A549 cells with TGF-β_1 and luteolin, these effects were much reduced and a part of the cells retained an epithelial morphology (**Figure 4A**). Immunoblot for E-cadherin, fibronectin, and vimentin (**Figure 4B**) reflected the morphological findings (**Figure 4A**) and showed features of EMT in A549 cells treated with TGF-β_1 with reduction in E-cadherin and induction of fibronectin and vimentin (**Figure 4B**). Interestingly, luteolin strikingly blocked TGF-β_1-mediated E-cadherin reduction and fibronectin induction, while the expression of basal and TGF-β_1-induced vimentin with no statistical difference (**Figure 4B**).

To investigate if luteolin inhibits TGF-β_1-induced alveolar EMT via the same signaling pathway in rodent and human, we examined the expression of total and phosphorylated Smad2/3 in A549 cells. As the same result in primary mouse lung fibroblasts, the increased expression of phosphorylated Smad2/3, but not total Smad2/3, by TGF-β1 was suppressed by pretreatment with luteolin in A549 cells (**Figures 4C**). No significant cytotoxic effect was observed after incubation with 5 to 50 μM luteolin for 48 h (**Figure 4D**).

DISCUSSION

The current study showed that luteolin effectively alleviated lung damage induced by intratracheal instillation of bleomycin in mice. This beneficial effect was based on the improvement of early inflammatory changes as well as on the late fibrotic formation. Treatment with luteolin clearly reduced the biochemical and histological signs of lung inflammation and fibrosis including collagen content, and some inflammatory and fibrogenic cytokines such as TNF-α, IL-6, and TGF-β_1. Additionally, our *in vitro* studies reveal that luteolin suppressed TGF-β_1-induced EMT by increase of epithelial marker E-cadherin expression and decrease of myofibroblast markers, α-SMA, collagen I,

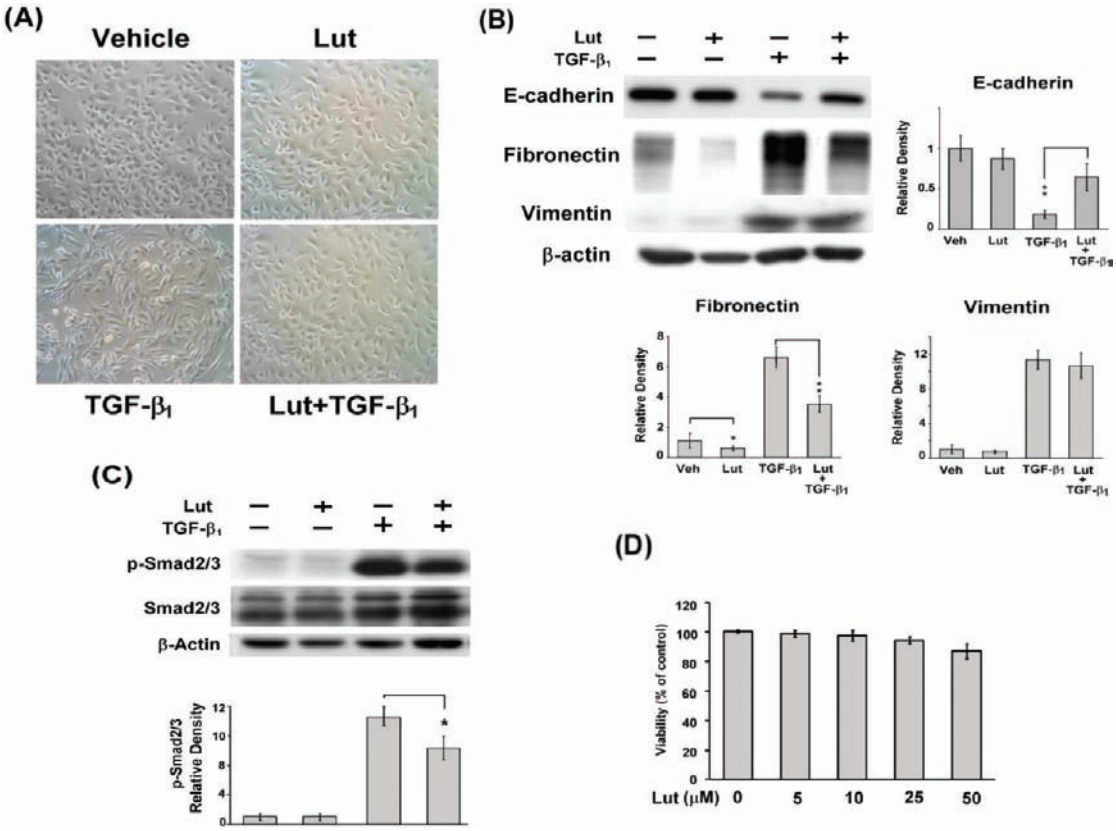

Figure 4. Inhibition of TGF-β1-induced EMT by luteolin in A549 cells. (**A**) Morphological change. Serum-starved A549 cells were incubated with TGF-β1 (5 ng/mL) in the absence or presence of luteolin (25 μM) for 48 h, the morphological change was microphotographed using Olympus IX70 microscope (magnification 200×). (**B**) Expression of EMT-related markers. A549 cells were treated as described above. The expression of E-cadherin, fibronectin and vimentin was observed by Western blot analysis. (**C**) Decrease of TGF-β1-induced Smad3 phosphorylation by luteolin in A549 cells. Cells were pretreated with luteolin (25 μM) for 30 min, and then treated with TGF-β1 (5 ng/mL) for another 30 min. Phosphorylation and total Smad2/3 were measured by Western blot analysis using antibodies against phospho-Smad2/3 and Smad2/3. The blots were analyzed by densitometry and the results expressed as relative units. Data from triplicate experiments are shown as mean ± SD. $^{*}p < 0.05$, $^{**}p < 0.01$.

fibronectin, and vimentin expression in primary cultured mouse lung fibroblasts and human alveolar epithelial-derived A549 cells.

Accumulating evidence demonstrates that the pathogenesis of idiopathic lung fibrosis begins with alveolitis characterized by accumulation of inflammatory cells. Neutrophils and mononuclear cells accumulate, and concomitant cytokines (like TGF-β_1) are released to stimulate fibroblast proliferation and migration into the areas of acute lung injury and stimulated to secrete collagen and other matrix proteins (*18*). In assessment of the effects of luteolin on the pulmonary inflammatory phase *in vivo*, we found that the increase in the number of inflammatory cells in the BAL fluid on day 7 after bleomycin injection was significantly attenuated by luteolin (**Table 1**). Luteolin also reduced the production of IL-6 and TNF-α (**Figure 1**). Our findings suggest the possibility that luteolin inhibits the migration of neutrophils into the airspace, which would be an important anti-inflammatory mechanism in this model. TNF-α, IL-6, and TGF-β_1 released from activated alveolar immune cells have been strongly implicated in the pathogenesis of human and experimental lung fibrosis (*19*). Here, we found that luteolin blocked bleomycin-induced TNF-α, IL-6, and TGF-β_1 expression. A previous report also indicates that luteolin protects against LPS-induced acute inflammation and lethal toxicity, possibly by inhibiting pro-inflammatory molecule (TNF-α, ICAM-1) expression in vivo and reducing leukocyte infiltration in tissues (*20*). Our previous study shows that luteolin can inhibit LPS-induced TNF-α, IL-6, iNOS, and COX-2 expression in both mouse macrophage RAW264.7 and MH-S cell lines (*11*). Consistently, several *in vitro* studies demonstrate that luteolin can suppress TNF-α, IL-6 and TGF-β_1 expression in different types of cells. For instance, lutoelin inhibits the expression of TNF-α, IL-6, and IL-12 in activated macrophages (*21*); treatment with luteolin decreases the expression of IL-6, IL-8, IL-15, and TGF-β_1 in stimulated rat synovial fibroblasts (*22*). Anti-inflammatory agents such as nonsteroidal anti-inflammatory drugs and corticosteroids, cytokines and antioxidants also exhibit antifibrotic activity in bleomycin-induced lung fibrosis model (*23*, *24*). Therefore, we hypothesize that the anti-inflammatory activity may be the mechanism of the antifibrotic effect of early treatment with luteolin.

In this study, the protective effect of luteolin was compared to that of prednisolone, which is used as first-line therapy for the treatment of patients with idiopathic pulmonary fibrosis (*25*). However, its clinical efficacy is equivocal. The timing for initiation of treatment is likely to be a crucial factor for corticosteroids to exert an antifibrotic effect. Our studies in animals show that early treatment with luteolin or prednisolone (starting at day 1) significantly ameliorated lung fibrosis induced by bleomycin. The striking suppression of bleomycin-induced lung fibrosis in mice treated with the delayed luteolin administration (starting at day 10) indicates that luteolin may be able to inhibit an ongoing fibrosis (**Figure 2**); however, delayed prednisolone treatment failed to suppress lung fibrosis. Our data indicate that although prednisolone has anti-inflammatory activity, and therefore a slight reducing lung fibrosis, luteolin has a much greater anti-inflammatory activity as well as antifibrotic activity than prednisolone. Although the level of TGF-β_1 was less in delayed

luteolin treatment than that in early luteolin treatment (**Figure 2D**), the reduction of the TGF-β_1 level in delayed luteolin treatment did not reach statistical significance when compared to that in early luteolin treatment. The difference might be caused by individual difference of mice. Overall, these observations suggest that the mechanical action of luteolin against bleomycin-induced lung fibrosis in mice may involve not only anti-inflammatory effect but also antifibrotic effect. A previous study showed that luteolin has therapeutic effects on CCl_4-induced liver fibrosis by promoting extracellular matrix degradation in the fibrotic liver tissue (*26*). Our ongoing study also showed that luteolin suppressed TGF-β1-induced MMP2 and MMP9 expression in both primary cultured mouse lung fibroblasts and the A549 cell line (data not shown); we suppose that luteolin should have the same effects on the prevention of lung fibrosis. Additional studies are required to specify further the main mechanism(s) of the beneficial effect of luteolin in this model as well as the potential for luteolin administration as concomitant therapy for patients with fibrotic alveolitis.

Lung fibrotic disorders are characterized by complex and dynamic interactions between regenerating/reparative epithelial cells and activated myofibroblasts (*27*). Increasing proliferation of resident fibroblasts, fibroblast-myofibroblast transdifferentiation, and extracellular matrix accumulation are central to fibrosis in all tissues (*28*). In our *in vitro* study, luteolin effectively inhibited cell proliferation and promoted myofibrobalst-like differentiation of primary cultured mouse lung fibroblasts (**Figure 3**). Immunocytochemical and immunoblotting analysis show that the expression of basal and TGF-β1-induced mesenchymal markers, including α-SMA, collagen I and vimentin, was significantly reduced in luteolin-treated lung fibroblasts. Although expansion of resident fibroblasts likely occurs in response to injury, several lines of evidence support the possibility that lung fibroblast development during injury responses may also be derived from bone marrow and/or epithelial cells (*29*). There have been prior suggestions that EMT occurs in the lung during fibrogenesis and TGF-β_1 plays an important role in promoting this event (*12*). During EMT, the intercellular adhesion molecule E-cadherin appears to have a central role, since the loss of E-cadherin expression correlates with the ability of epithelial cells to adopt mesenchymal phenotypes (*30*). TGF-β_1 treatment has been shown to alter the cell morphology of the human alveolar type II epithelial cell-derived A549 cell line from cobblestone-shaped to a fibroblastoid appearance. This cell line is commonly used for study on the role of human alveolar type II epithelial cells as they retain features and metabolic properties characteristic of type II cells (*31*). Similarly, we found that exposure of A549 cells to TGF-β_1 induced EMT characterized by loss of epithelial marker E-cadherin, transdifferentiating to the mesenchymal-like phenotype, and increasing of mesenchymal marker fibronectin, which, however were inhibited by luteolin (**Figure 4**). Although the reduction of vimentin by luteolin at 25 μM though not as obvious as that in fibroblasts (**Figure 4B**). However, the expressed level of vimentin was markedly suppressed after 40 μM luteolin treatment (data not shown). This evidence suggesting that luteolin inhibited potent phenotypic alterations induced by TGF-β_1 would predictably augment alveolar re-epithelialization in vivo.

TGF-β_1 signaling from the cell membrane to the nucleus occurs mainly via Smad proteins. Smad2 and Smad3 are structurally highly similar and mediate TGF-β1 signals (*32*). It has been reported that Smad3 contributes to bleomycin-induced lung injury and is a major component of the signal transduction pathway leading to fibrogenesis (*33*). TGF-β_1-mediated EMT in A549 cells is thought to be dependent on Smad2 and Smad3 phosphorylation (*12*). With the same result in our study, expression of phosphorylated Smad2/3 by TGF-β1 in A549 cells was obvious. Luteolin also suppressed the phosphorylation of Smad2/3. It indicated that the mechanisms for the potent luteolin-dependent inhibitory effects observed for myofibroblast differentiation were the same with EMT in A549 cells (**Figures 3C** and **4B**).

In conclusion, this is the first study that convincingly demonstrates that treatment with luteolin markedly alleviated bleomycin-induced lung inflammation and fibrosis in mice by inhibiting TNF-α, IL-6, TGF-β_1, α-SMA, and collagen I expression. Luteolin was generally more effective than prednisolone. The *in vitro* studies reveal that luteolin could suppress TGF-β_1-induced fibroblast-to-myofibroblast differentiation and epithelial-to-mesenchymal transition by increase in expression of epithelial marker (E-cadherin) and decrease in mesenchymal markers (α-SMA and collagen I) in primary cultured mouse lung fibroblasts and alveolar epithelial-derived A549 cells. Due to the lack of effective therapy to inhibit the progression of lung fibrosis, these findings support further exploration of the antifibrotic properties and mechanisms of action of luteolin in both *in vivo* and *in vitro* models to clarify its potential therapeutic benefit.

ABBREVIATIONS USED

ILDs, interstitial lung diseases; EMT, epithelial-to-mesenchymal transition; BALF, bronchoalveolar lavage fluid; RT-PCR, reverse transcriptase-polymerase chain reaction.

LITERATURE CITED

(1) King, T. E., Jr. Clinical advances in the diagnosis and therapy of the interstitial lung diseases. *Am. J. Respir. Crit. Care Med.* **2005**, *172* (3), 268−79.

(2) Gharaee-Kermani, M.; Phan, S. H. Molecular mechanisms of and possible treatment strategies for idiopathic pulmonary fibrosis. *Curr. Pharm. Des.* **2005**, *11* (30), 3943−71.

(3) Hashimoto, S.; Gon, Y.; Takeshita, I.; Matsumoto, K.; Maruoka, S.; Horie, T. Transforming growth Factor-beta1 induces phenotypic modulation of human lung fibroblasts to myofibroblast through a c-Jun-NH2-terminal kinase-dependent pathway. *Am. J. Respir. Crit. Care Med.* **2001**, *163* (1), 152−7.

(4) Dempsey, O. J. Clinical review: idiopathic pulmonary fibrosis--past, present and future. *Respir. Med.* **2006**, *100* (11), 1871−85.

(5) Izbicki, G.; Segel, M. J.; Christensen, T. G.; Conner, M. W.; Breuer, R. Time course of bleomycin-induced lung fibrosis. *Int. J. Exp. Pathol.* **2002**, *83* (3), 111−9.

(6) Shimabukuro, D. W.; Sawa, T.; Gropper, M. A. Injury and repair in lung and airways. *Crit .Care Med.* **2003**, *31* (8 Suppl.), S524−31.

(7) Lew, T. W.; Kwek, T. K.; Tai, D.; Earnest, A.; Loo, S.; Singh, K.; Kwan, K. M.; Chan, Y.; Yim, C. F.; Bek, S. L.; Kor, A. C.; Yap, W. S.; Chelliah, Y. R.; Lai, Y. C.; Goh, S. K. Acute respiratory distress syndrome in critically ill patients with severe acute respiratory syndrome. *JAMA, J. Am. Med. Assoc.* **2003**, *290* (3), 374−80.

(8) Lopez-Lazaro, M. Distribution and biological activities of the flavonoid luteolin. *Mini-Rev. Med. Chem.* **2009**, *9* (1), 31−59.

(9) Das, M.; Ram, A.; Ghosh, B. Luteolin alleviates bronchoconstriction and airway hyperreactivity in ovalbumin sensitized mice. *Inflammation Res.* **2003**, *52* (3), 101−6.

(10) Tormakangas, L.; Vuorela, P.; Saario, E.; Leinonen, M.; Saikku, P.; Vuorela, H. In vivo treatment of acute Chlamydia pneumoniae infection with the flavonoids quercetin and luteolin and an alkyl gallate, octyl gallate, in a mouse model. *Biochem. Pharmacol.* **2005**, *70* (8), 1222−30.

(11) Chen, C. Y.; Peng, W. H.; Tsai, K. D.; Hsu, S. L. Luteolin suppresses inflammation-associated gene expression by blocking NF-kappaB and AP-1 activation pathway in mouse alveolar macrophages. *Life Sci.* **2007**, *81* (23−24), 1602−14.

(12) Kasai, H.; Allen, J. T.; Mason, R. M.; Kamimura, T.; Zhang, Z. TGF-beta1 induces human alveolar epithelial to mesenchymal cell transition (EMT). *Respir. Res.* **2005**, *6*, 56.

(13) Kapoun, A. M.; Gaspar, N. J.; Wang, Y.; Damm, D.; Liu, Y. W.; O'Young, G.; Quon, D.; Lam, A.; Munson, K.; Tran, T. T.; Ma, J. Y.; Murphy, A.; Dugar, S.; Chakravarty, S.; Protter, A. A.; Wen, F. Q.; Liu, X.; Rennard, S. I.; Higgins, L. S. Transforming growth factor-beta receptor type 1 (TGFbetaRI) kinase activity but not p38 activation is required for TGFbetaRI-induced myofibroblast differentiation and profibrotic gene expression. *Mol. Pharmacol.* **2006**, *70* (2), 518−31.

(14) Khalil, N.; O'Connor, R. N.; Unruh, H. W.; Warren, P. W.; Flanders, K. C.; Kemp, A.; Bereznay, O. H.; Greenberg, A. H. Increased production and immunohistochemical localization of transforming growth factor-beta in idiopathic pulmonary fibrosis. *Am. J. Respir. Cell Mol. Biol.* **1991**, *5* (2), 155−62.

(15) Vaughan, M. B.; Howard, E. W.; Tomasek, J. J. Transforming growth factor-beta1 promotes the morphological and functional differentiation of the myofibroblast. *Exp. Cell Res.* **2000**, *257* (1), 180−9.

(16) Venkatesan, N.; Pini, L.; Ludwig, M. S. Changes in Smad expression and subcellular localization in bleomycin-induced pulmonary fibrosis. *Am. J. Physiol.* **2004**, *287* (6), L1342−7.

(17) Willis, B. C.; Borok, Z. TGF-beta-induced EMT: mechanisms and implications for fibrotic lung disease. *Am. J. Physiol.* **2007**, *293* (3), L525−34.

(18) Dhainaut, J. F.; Charpentier, J.; Chiche, J. D. Transforming growth factor-beta: a mediator of cell regulation in acute respiratory distress syndrome. *Crit. Care Med.* **2003**, *31* (4 Suppl.), S258−64.

(19) Zhang, Y.; Lee, T. C.; Guillemin, B.; Yu, M. C.; Rom, W. N. Enhanced IL-1 beta and tumor necrosis factor-alpha release and messenger RNA expression in macrophages from idiopathic pulmonary fibrosis or after asbestos exposure. *J. Immunol.* **1993**, *150* (9), 4188−96.

(20) Kotanidou, A.; Xagorari, A.; Bagli, E.; Kitsanta, P.; Fotsis, T.; Papapetropoulos, A.; Roussos, C. Luteolin reduces lipopolysaccharide-induced lethal toxicity and expression of proinflammatory molecules in mice. *Am. J. Respir. Crit. Care Med.* **2002**, *165* (6), 818−23.

(21) Lee, J. K.; Kim, S. Y.; Kim, Y. S.; Lee, W. H.; Hwang, D. H.; Lee, J. Y. Suppression of the TRIF-dependent signaling pathway of Toll-like receptors by luteolin. *Biochem. Pharmacol.* **2009**, *77* (8), 1391−400.

(22) Hou, Y.; Wu, J.; Huang, Q.; Guo, L. Luteolin inhibits proliferation and affects the function of stimulated rat synovial fibroblasts. *Cell Biol. Int.* **2009**, *33* (2), 135−47.

(23) Daniels, C. E.; Wilkes, M. C.; Edens, M.; Kottom, T. J.; Murphy, S. J.; Limper, A. H.; Leof, E. B. Imatinib mesylate inhibits the profibrogenic activity of TGF-beta and prevents bleomycin-mediated lung fibrosis. *J. Clin. Invest.* **2004**, *114* (9), 1308−16.

(24) Serrano-Mollar, A.; Closa, D.; Prats, N.; Blesa, S.; Martinez-Losa, M.; Cortijo, J.; Estrela, J. M.; Morcillo, E. J.; Bulbena, O. In vivo antioxidant treatment protects against bleomycin-induced lung damage in rats. *Br. J. Pharmacol.* **2003**, *138* (6), 1037−48.

(25) Dik, W. A.; McAnulty, R. J.; Versnel, M. A.; Naber, B. A.; Zimmermann, L. J.; Laurent, G. J.; Mutsaers, S. E. Short course dexamethasone treatment following injury inhibits bleomycin induced fibrosis in rats. *Thorax* **2003**, *58* (9), 765−71.

(26) Domitrovic, R.; Jakovac, H.; Tomac, J.; Sain, I. Liver fibrosis in mice induced by carbon tetrachloride and its reversion by luteolin. *Toxicol. Appl. Pharmacol.* **2009**, *241* (3), 311−21.

(27) Thannickal, V. J.; Toews, G. B.; White, E. S.; Lynch, J. P., 3rd; Martinez, F. J. Mechanisms of pulmonary fibrosis. *Annu. Rev. Med.* **2004**, *55*, 395−417.

(28) Desmouliere, A.; Chaponnier, C.; Gabbiani, G. Tissue repair, contraction, and the myofibroblast. *Wound Repair Regen.* **2005**, *13* (1), 7−12.

(29) Phillips, R. J.; Burdick, M. D.; Hong, K.; Lutz, M. A.; Murray, L. A.; Xue, Y. Y.; Belperio, J. A.; Keane, M. P.; Strieter, R. M. Circulating fibrocytes traffic to the lungs in response to CXCL12 and mediate fibrosis. *J. Clin. Invest.* **2004**, *114* (3), 438−46.

(30) Kim, J. H.; Jang, Y. S.; Eom, K. S.; Hwang, Y. I.; Kang, H. R.; Jang, S. H.; Kim, C. H.; Park, Y. B.; Lee, M. G.; Hyun, I. G.; Jung, K. S.; Kim, D. G. Transforming growth factor beta1 induces epithelial-to-mesenchymal transition of A549 cells. *J. Korean Med. Sci.* **2007**, *22* (5), 898−904.

(31) Foster, K. A.; Oster, C. G.; Mayer, M. M.; Avery, M. L.; Audus, K. L. Characterization of the A549 cell line as a type II pulmonary epithelial cell model for drug metabolism. *Exp. Cell Res.* **1998**, *243* (2), 359−66.

(32) Massague, J.; Wotton, D. Transcriptional control by the TGF-beta/Smad signaling system. *EMBO J.* **2000**, *19* (8), 1745−54.

(33) Bonniaud, P.; Kolb, M.; Galt, T.; Robertson, J.; Robbins, C.; Stampfli, M.; Lavery, C.; Margetts, P. J.; Roberts, A. B.; Gauldie, J. Smad3 null mice develop airspace enlargement and are resistant to TGF-beta-mediated pulmonary fibrosis. *J. Immunol.* **2004**, *173* (3), 2099−108.

Received for review August 15, 2010. Revised manuscript received October 5, 2010. Accepted October 5, 2010. This work was supported in part by grants from the Taichung Veterans General Hospital (TCVGH987323D), Taichung Veterans General Hospital and National Chi Nan University (TCVGH-NCNU987901), and National Science Council (Taiwan) (NSC95-2320-B-075A-002-MY3) to S.-L.H., and National Science Council (Taiwan) NSC98-2320-B-343-001 to C.-Y.C.